Heliyon 6 (2020) e03165

Contents lists available at ScienceDirect

Heliyon

journal homepage: www.cell.com/heliyon

Research article

Durability of self-consolidating concrete containing natural waste perlite powders

Abdulkader El Mir [a], Salem G. Nehme [b], Joseph J. Assaad [a,*]

[a] University of Balamand, Al Kourah, Lebanon
[b] Laboratory and Associate Professor, Budapest University of Technology and Economics, Budapest, Hungary

ARTICLE INFO

Keywords:
Civil engineering
Construction engineering
Cement additive
Concrete structure
Cement
Physical property
Waste perlite
Self-consolidating concrete
Durability
Transport properties
Freeze/thaw
Permeability

ABSTRACT

Perlite is a natural glassy volcanic rock used in construction applications requiring improved lightweight, thermal, and acoustic properties. During processing of raw perlite (i.e., cutting and fractioning to different sizes), large amounts of powders are collected and stored as waste materials. This paper evaluates the effect of waste perlite (WP) powders on durability and long-term transport properties of self-consolidating concrete (SCC). Different mixtures prepared with 580 kg/m^3 powder using various combinations of WP, limestone filler (LF), metakaolin (MK), and silica fume (SF) are tested over 2-years period. Test results showed that WP confers particular benefits to the SCC compressive strength and its evolution over time, particularly when used in combination with MK and SF. Water permeability, carbonation, and chloride ion migration curtailed when WP concentration reached 220 and 260 kg/m^3. In contrast, the resistance against freeze/thaw remarkably improved, given the pozzolanic reactions and porous nature of such powders that accommodated the disruptive expansive stresses resulting from frost attack.

1. Introduction

The development of self-consolidating concrete (SCC) requires relatively high amounts of powder materials to secure adequate stability on the fresh state as well as optimized performance and durability of the hardened product [1, 2, 3]. Properly selected powders (whether or not possessing pozzolanic activity) can enhance cohesiveness and inter-particle links in the cementitious system, leading to improved resistance against bleeding and coarse aggregate segregation. Increasing the powder content also increases the paste volume, which indirectly reduces mixing water required to achieve high deformability [2, 4, 5]. This can offset the need for viscosity-modifying admixtures, while ensuring adequate stability and strength isotropy of the cast elements.

On the hardened state, the addition of pozzolanic powders such as silica fume (SF), metakaolin (MK), fly ash (FA), and blast furnace slag (BFS) was reported to produce stronger and denser SCC microstructure and interfacial zones around coarse aggregates and embedded reinforcing bars [6, 7, 8]. Zhu and Bartos [9] reported significant resistance to oxygen permeability, capillary water absorption, and chloride diffusion for SCC mixtures containing different combinations of pulverized FA, when compared to control concrete having similar compressive strengths of 40–60 MPa. Hwang and Khayat [10] showed that the type of binder has considerable influence on the pore-size distribution, rapid-chloride penetration (RCP), and chloride diffusion coefficients. The SCC prepared with quaternary binder composed of cement (CEM), SF, FA, and BFS developed 60%–80% lower RCP values, 40% lower chloride diffusion, and 15%–25% lower porosity than other mixtures made with binary blended cements [10]. Sujjavanich et al. [8] showed that the resistance against abrasion, RCP, and steel corrosion can be significantly improved when combining 80% CEM with 10% FA and 10% MK. The synergistic action of the ternary blend yielded a cohesive concrete with denser microstructure [6, 8].

Limestone filler (LF) is readily available mineral powder that attracted concrete technologists during SCC proportioning [1, 11, 12]. Ghezal and Khayat [1] found that such additions can reduce the cost of SCC materials, while satisfying stringent performance criteria related to slump flow, rheology, and stability. Tested mixtures contained up to 120 kg/m^3 LF, 250–400 kg/m^3 CEM, and water-to-powder ratio (w/p) varying from 0.38 to 0.72. The LF is not reactive with calcium hydroxide; however, many studies proved its efficiency to promote nucleation and C-S-H precipitation during cement hydration [12, 13, 14]. Silva and Brito [6] reported that the substitution of CEM by large FA and/or LF volumes

* Corresponding author.
E-mail address: joseph.assaad@balamand.edu.lb (J.J. Assaad).

https://doi.org/10.1016/j.heliyon.2020.e03165
Received 14 July 2019; Received in revised form 23 October 2019; Accepted 31 December 2019

(i.e., up to 65%) can substantially alter the SCC pore structure and durability. The authors concluded that SCC produced with LF has lower total porosity but larger pores, while the opposite becomes true for mixtures containing FA (i.e., higher porosity but smaller pores). The use of ternary blends (i.e., CEM, FA, and LF) proved extremely favorable, confirming the beneficial synergistic effect between these additions [6]. Similar conclusions were drawn by Antoni et al. [15] who showed that ternary binders composed by CEM, MK, and LF lead to higher hydration rates and mechanical strengths than binary cements. However, this behavior was found to be highly affected by the mixture composition and physico-chemical properties of the powder materials [15, 16]. Medjigbodo et al. [17] reported that the equivalent strength of MK-based binary mixtures can be secured, provided that highly reactive MK is used and the replacement rate of CEM by MK does not exceed 30%. The authors showed evidence that higher substitution of CEM is possible by combining MK with LF; the presence of both additions improved packing density of the paste and fostered primary and secondary hydration reactions [17].

Perlite is a natural glassy volcanic rock located in several countries such as Turkey, Greece, Hungary, Japan, and USA [18, 19, 20]. When subjected to heat, perlite expands 5 to 20 times its original volume, making it suitable for various lightweight concrete applications, brick production, plasters, or constructional elements requiring improved thermal and acoustic insulations [21, 22]. Nevertheless, during processing of raw perlite (i.e., cutting, grinding, and fractioning to different sizes), large amounts of powders are collected and stored as waste materials. It is estimated that the waste perlite (WP) powder constitutes about 5%–10% of the original rock, having particle sizes ranging from few microns to about 0.5 mm [18, 20]. Presently, only limited amounts of WP is recycled in the construction industry, highlighting the need to efficiently manage such wastes and their impact on the environment.

Because of high SiO_2 and Al_2O_3 contents, perlite powders (whether used in natural state or calcined at high temperature) are pozzolanic materials that improve strength and durability of concrete mixtures [19, 23, 24]. Ramezanianpour et al. [25] reported that the incorporation of perlite consumes the lime and reduces conductivity of the cement pore solution due to pozzolanic reactions. Tested powders were obtained by calcining perlite rocks for 1 h at 850 °C, followed by grinding to reach similar fineness as the CEM. The perlite was more effective at longer curing periods as well as higher free mixing water, which was evidenced by reduced porosity and connectivity of pores due to additional C-S-H gel formations [25]. Bektas et al. [26] concluded that the incorporation of perlite could mitigate the expansion phenomenon resulting from alkali-silica reactions in concrete, albeit the calcined perlite seemed to be more effective than the natural one. This was attributed to a combination of phenomena including consumption of calcium hydroxide, decreased ionic mobility as a result of refined and less accessible pore structure, and binding of alkalis during cement hydration [26]. Yu et al. [27] reported that optimum compressive strength can be achieved when the CEM replacement by natural perlite does not exceed 15%–20%. Erdem et al. [24] demonstrated that the grinding of perlite was necessary to reduce water demand and enhance its pozzolanic activity; the improvement in compressive strength occurred when 95% of the powder perlite passed the 80-μm sieve. In contrast, the inclusion of coarse perlite particles characterized by open pores and inter-connected channels increased concrete vulnerability to water absorption, permeability, and chloride migration [24, 28].

Limited investigations evaluated the combined effects of natural WP together with LF, MK, and SF on durability and transport properties of highly flowable SCC. Different mixtures prepared with fixed powder content and w/p of 580 kg/m^3 and 0.31, respectively, are proportioned. Testing was conducted for 2-years period, and properties evaluated included compressive strength, porosity, water permeability, carbonation, chloride migration, and freeze/thaw resistance. Such data can be of particular interest to researchers and concrete practitioners seeking the efficient management and use of WP materials.

2. Experimental program

2.1. Materials

Portland cement complying with BS EN 197-1 requirements along with commercially available LF, MK, and SF materials are used in this study. The LF Blaine fineness and mean diameter size (d_{50}) for which 50% of the material is comprised of smaller particles were 3,480 cm^2/g and 6.5 μm, respectively [29]. The MK is produced by calcination of concentrated raw kaolin, then grinding to about 15,000 cm^2/g BET fineness. The SF had d_{50} and BET fineness of 0.6 μm and 20,450 cm^2/g, respectively.

The WP was collected during processing raw perlite rocks. It had relatively wide range of particle sizes that can be broadly divided into fine and coarse fractions (Figure 1). The coarse fraction contains about 20% of particles ranging from 40 to 150 μm; the overall Blaine finesses was 1,670 cm^2/g. The WP photomicrographs show, for some particles, the sharp edges resulting from the cutting process of the perlite rocks. The WP possessed a specific gravity of 2.33 determined as per ISO 17892-3 test [30], reflecting relatively porous texture as compared to LF, MK, and SF materials.

The particle size distributions of all powder materials (i.e., CEM, LF, MK, SF, and WP) are plotted in Figure 2, while their chemical and physical characteristics are summarized in Table 1. The 28-days strength activity index determined at 10% replacement rates for LF, MK, SF, and WP are 98.8%, 112.3%, 118.5%, and 104.8%, respectively.

Quartz sand (0/4 mm), small gravel (4/8 mm), and medium gravel (8/16 mm) were used; their fineness modulus, bulk specific gravity, and water absorption were 3.73/6.93/7.99, 2.62/2.63/2.67, and 1.1/1.73/2.1%, respectively. Polycarboxylate-type high-range water reducer (HRWR) complying with EN 934-2:2009 was used; its solid content and specific gravity were 35 and 1.08, respectively.

2.2. SCC mixture proportions

Twelve mixtures prepared with fixed powder content of 580 kg/m^3 and free mixing water of 180 kg/m^3 are tested; the resulting w/p was 0.31 (Table 2). The mixtures are divided in three categories, depending on the cement content. In the first category, the CEM was set at 400 kg/m^3, while WP or LF added at 180 kg/m^3 (this represents 31% of powder content). The resulting water-to-cement ratio (w/c) was 0.45. An amount of 40 kg/m^3 (i.e., 7% of powder) of either WP or LF was then replaced by MK or SF to determine the synergistic effects of such combinations on durability and transport properties (Table 2). The other two SCC categories are made with reduced cement content (i.e., 360 or 320 kg/m^3), which resulted in w/c of 0.5 and 0.56, respectively. The WP was added at either 220 or 260 kg/m^3, representing 38% and 45% of the powder content, respectively. As earlier, the MK and SF are incorporated at 40 kg/m^3. The sand-to-total aggregate ratio remained fixed at 0.45 for all mixtures.

The HRWR was adjusted in all mixtures to secure slump flow of 790 ±15 mm. The resulting Visual Stability Index (VSI) varied from 0.5 to 1.0, reflecting proper stability with minimum bleeding and segregation [1, 31, 32]. The VSI is a numerical rating varying from 0 to 3 (i.e., reflecting good to poor stability), assigned to the concrete texture after conducting the slump flow test [33].

2.3. Concrete batching

All mixtures were batched in open pan mixer of 100-L capacity. The mixing sequence consisted of homogenizing the fine and coarse aggregates together with about 50% of mixing water for 30 s in the mixer. The powders were then added with the rest of water, followed by HRWR, and concrete mixed for two minutes. After conducting the slump flow, the mixing was resumed for 1 additional minute. The temperature of fresh mixtures was kept around 23 ±2 °C.

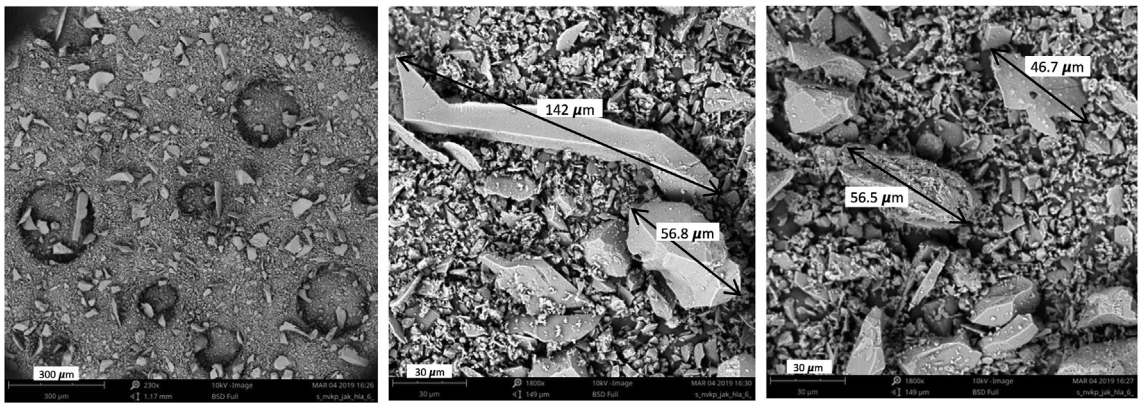

Figure 1. Photomicrographs for WP materials at magnifications of 300-μm (left part) and 30-μm (middle and right parts).

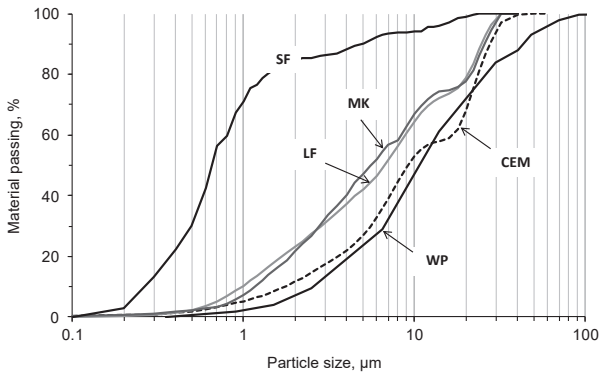

Figure 2. Particle size distribution curves for various powder materials.

2.4. Test methods

Following the end of mixing, the slump flow diameter and V-Funnel flow time were determined (Table 2), as per EFNARC guidelines for SCC [33]. The fresh mixtures were then cast in 150-mm cubic molds or 100×200-mm cylinders for testing hardened properties. The specimens were demolded after 24 h, immersed in water for 7 days, then conserved in a room where ambient temperature and relative humidity remained within 23 ±3 °C and 50 ±10%, respectively.

The compressive strength (f'_c) of investigated mixtures was determined on cubic specimens, as per BS EN 12390-3 Test Method [34]. Testing was made after 7, 28, 90, 400, and 600 days; averages of 3 cubes are considered for each measurement. Total porosity of hardened SCC was evaluated as the ratio between densities of bulk concrete with respect to the discrete particles [35]. Portions of hardened specimens were crushed and ground finer than 0.02 mm, so that no impermeable pore space can exist within the particles. The density of discrete particles was determined by pycnometer method using oven-dried materials. Three specimens for each mixture aged at 400 days are used.

The water permeability was determined following BS 1881-122 and EN 12390-8 Test Methods [36, 37]. In the former test, the 100×200-mm cylinders were oven-dried, then immersed in water for 24 h to determine the percent increase in specimen mass (or, water absorption rate (W_{abs}, %)). In the second test, the 150-mm cubic specimens were subjected to 5 bar of water pressure for a period of 72 h. The specimens were then splitted in half to visualize and measure the depth of water penetration (W_{depth}, mm). Three specimens are considered for each test, and measurements made after 90 and 650 days. Table 3 summarizes the density of hardened specimens, f'_c, W_{abs}, and W_{depth} determined at various ages.

The transport properties including carbonation depth (D_{carb}) and chloride migration coefficient (D_{nssm}) were evaluated according to RILEM CPC-18 and Nordtest Method NT Build 492, respectively [38, 39]. The concrete slices were exposed to ambient (about 0.05%) carbon dioxide to evaluate D_{carb}; three 45 × 150 × 150-mm sized specimens were tested at each time interval of 28, 90, 400, and 600 days. A solution of 1% phenolphthalein diluted in 70% ethyl alcohol was sprayed on cross sections to determine the depth of carbonated concrete [38]. For D_{nssm} measurements, concrete slices having 50-mm thickness and 100-mm diameter are used; these were vacuumed and saturated in water for 7 days prior to testing. The visualization of the chloride penetration depth was made by colorimetry using 0.1 M silver nitrate ($AgNO_3$) solution sprayed on the split specimen surfaces [39]. The D_{nssm} measurements were performed after 28, 90, and 460 days. Table 4 summarizes the D_{carb} and D_{nssm} at various ages.

The SCC internal damage due to freeze-thaw (F/T) cycles was determined using 150-mm saturated cubes having 90 days of age [40]. The F/T cycles consisted of alternately lowering the water temperature to –20 ±4 °C in 4 h, then thawing at +20 ±4 °C for another 4 h. An aqueous solution containing 3% sodium chloride (NaCl) was used. The loss of mass as well as change in ultrasonic pulse velocity at 54-kHz frequency were recorded up to 400 F/T cycles, in an offset of 50 cycles [41]. A durability factor (DF) was determined as $(V_n/V_0)^2$, where V_n and V_0 refer to pulse velocity measured after n F/T cycles and the one measured before beginning of the test cycles, respectively. At end of the last cycle (i.e., number 400), the concrete cube was tested in compression (Table 5).

Table 1. – Chemical and physical properties of CEM, WP, LF, MK, and SF.

	CEM	WP	LF	MK	SF
SiO_2, %	25.53	73.5	5.63	52.79	95.09
Al_2O_3, %	6.3	14.4	1.4	42.07	0.24
Fe_2O_3, %	2.29	1.96	0.9	1.25	0.06
CaO, %	55.59	1.11	50.32	0.37	0.91
MgO, %	4.05	0.15	0.65	0.38	0.32
SO_3, %	2.34	-	0.08	<0.01	0.07
K_2O, %	0.78	3.76	0.29	1.22	0.51
Na_2O, %	0.33	2.12	0.07	0.02	0.2
TiO_2, %	0.28	0.086	0.08	0.2	<0.01
P_2O_5, %	0.03	-	0.02	0.06	0.07
Specific gravity	3.1	2.33	2.69	2.6	2.35
Surface area, cm^2/g	3,400	1,670	3,480	15,000	20,450
Loss On Ignition, %	2.15	1.87	40.55	1.59	2.49
Strength activity index, %	n/a	104.8	98.8	112.3	118.5

3. Test results and discussion

3.1. HRWR demand and V-Funnel flow times

As summarized in Table 2, the LF-based mixtures prepared with 400 kg/m^3 cement required around 2 to 3-times less HRWR, than

Table 2. – Mixture composition for tested SCC.

	Powder materials, kg/m^3					Agg., L/m^3	w/p	w/c	HRWR, L/m^3	Slump flow, mm	V-Funnel, sec
	CEM	WP	LF	MK	SF						
400C-180WP	400	180	-	-	-	592	0.31	0.45	7.9	790	7.9
400C-140WP-40MK	400	140	-	40	-	593	0.31	0.45	8.4	765	11.7
400C-140WP-40SF	400	140	-	-	40	591	0.31	0.45	8.8	790	8
400C-180LF	400	-	180	-	-	607	0.31	0.45	2.7	780	4.6
400C-140LF-40MK	400	-	140	40	-	605	0.31	0.45	4	810	8.6
400C-140LF-40SF	400	-	140	-	40	604	0.31	0.45	3.7	790	5.1
360C-220WP	360	220	-	-	-	588	0.31	0.5	7.5	800	5.5
360C-180WP-40MK	360	180	-	40	-	589	0.31	0.5	8.1	790	8.1
360C-180WP-40SF	360	180	-	-	40	587	0.31	0.5	7.9	770	6.4
320C-260WP	320	260	-	-	-	584	0.31	0.56	6.4	785	6.1
320C-220WP-40MK	320	220	-	40	-	585	0.31	0.56	7.4	800	8.6
320C-220WP-40SF	320	220	-	-	40	584	0.31	0.56	7	785	5.5

Note: The powder and water contents are fixed at 580 and 180 kg/m^3, respectively.

Table 3. – Compressive strength, porosity, and water permeability.

	Density, kg/m^3	f_c, MPa				Porosity, %	W_{abs}, %		W_{depth}, mm
	90 d	28 d	90 d	400 d	600 d	400 d	90 d	650 d	90 d
400C-180WP	2323	76.5	90.9	105.2	110.7	6.34	4.42	1.77	9.27
400C-140WP-40MK	2376	86.4	98.1	115.7	119.3	6.02	2.72	1.51	8.4
400C-140WP-40SF	2342	78.4	94.2	110.3	113.3	6.25	1.75	1.27	3.2
400C-180LF	2345	57.7	63.2	76.2	79.5	11.2	3.12	n/a	12.24
400C-140LF-40MK	2339	69.9	78.1	90.2	95	8.98	1.84	1.41	7.58
400C-140LF-40SF	2361	70.5	82.3	91.6	94.5	9.06	1.72	n/a	5.9
360C-220WP	2317	62.9	77	101	103.4	n/a	4.13	3.65	11.01
360C-180WP-40MK	2340	74	89.7	106.3	109.5	n/a	3.54	2.84	11.56
360C-180WP-40SF	2323	74.8	86.6	100.5	109.6	6.89	3.21	2.53	9.23
320C-260WP	2269	52.9	66.9	87.3	91.9	11.11	6.12	4.63	14.78
320C-220WP-40MK	2301	61.9	72.1	90.2	93.5	8.63	3.96	3.34	15.41
320C-220WP-40SF	2291	62.8	79.2	93.7	96.5	n/a	3.41	3.06	9.78

corresponding SCC made with WP. For instance, the HRWR increased from 2.7 to 7.9 L/m^3 for the 400C-180LF and 400C-180WP mixtures, respectively. This may partly be attributed to the relatively WP porous texture (compared to LF), which could absorb part of mixing water with consequent increase in HRWR demand [20, 28]. Such observation concurs with published data related to porous materials such as lightweight and recycled aggregates [19, 42, 43].

Table 4. – Transport properties (i.e., D_{carb} and D_{nssm} measurements).

	D_{carb}, mm				$D_{nssm} \times 10^{-12}$, m^2/s		
	28 d*	90 d	400 d	600 d	28 d	90 d	460 d
400C-180WP	0.4	0.91	2.41	5.05	5.25	3.01	2.63
400C-140WP-40MK	0.4	0.54	1.9	4.1	4.31	3.09	2.06
400C-140WP-40SF	0.4	0.6	2.23	3.91	4.94	2.49	1.54
400C-180LF	0.55	0.72	2.81	5.2	5.52	2.98	2.41
400C-140LF-40MK	0.35	0.66	2.3	4.61	3.71	2.5	1.57
400C-140LF-40SF	0.4	0.62	2.05	3.93	2.52	1.25	n/a
360C-220WP	0.65	0.81	3.14	5.92	6.8	5.16	3.81
360C-180WP-40MK	0.6	0.72	2.26	4.82	5.43	4.85	3.49
360C-180WP-40SF	0.55	0.63	2.1	4.6	5.66	4.49	3.12
320C-260WP	0.7	1.04	3.24	6.31	11.01	6.76	4.15
320C-220WP-40MK	0.65	0.91	2.92	5.75	7.53	5.97	4.12
320C-220WP-40SF	0.65	1.05	2.81	5.53	5.99	4.51	2.94

* D_{carb} values at 28 days were rounded to the nearest 0.05 mm.

The HRWR demand slightly increased when 40 kg/m^3 WP was replaced by MK or SF (Table 2). For example, at 400 kg/m^3 cement, the HRWR increased from 7.9 L/m^3 for the 400C-180WP mixture to 8.4 and 8.8 L/m^3 with the addition of MK and SF, respectively. This can be related to higher MK and SF fineness, requiring additional HRWR molecules to lubricate the powder materials and secure the targeted workability [4, 31]. The flow times for all mixtures varied between 5 and 12 s, reflecting adequate passing ability through the tapered outlet of the V-Funnel apparatus [5, 31].

3.2. Compressive strength and its evolution over time

Figure 3 plots the compressive strengths determined after 28 days for tested mixtures as well as their evolutions over curing time (i.e., $\Delta(f_c)$). The $\Delta(f_c)$ is calculated as the ratio between f_c measured after given elapsed time minus $f_{c(28d)}$, divided by $f_{c(28d)}$, and multiplied by 100. For given CEM content, mixtures containing WP exhibited remarkably higher $f_{c(28d)}$ than those prepared using LF; for example, the $f_{c(28d)}$ dropped from 76.5 to 57.7 MPa for the 400C-180WP and 400C-180LF mixtures, respectively. This contrasting change in strength can be associated to different physico-chemical compositions and interactions during cement hydration and phase development [12, 16, 24]. In fact, WP is an alumino-silicate rich powder that reacts with Portlandite during hydration and forms additional C-S-H and C-A-S-H rigid compounds, while in contrast, LF is a chemically inert filler. Thermogravimetric analysis performed by Antoni et al. [15] showed higher amounts of Portlandite in

Table 5. – Freeze/Thaw measurements after 90 days.

	V_0, m/s	E, GPa	DF, %		Cum. mass loss, %		f'_c after last F/T cycle, MPa
			After 300 cycles	After 400 cycles	After 300 cycles	After 400 cycles	
400C-180WP	4.69	52.1	86	77.2	1.25	1.84	77.9
400C-140WP-40MK	4.75	54.7	84	67.4	1.82	2.73	53.5
400C-140WP-40SF	4.765	54.2	93.3	93.1	1.24	1.74	90.4
400C-180LF	4.495	48.3	95	79.2	1.17	1.68	51.5
400C-140LF-40MK	4.72	53.1	87.3	66.5	1.79	2.63	59.2
400C-140LF-40SF	4.73	53.9	93.4	85	1.18	1.57	76.4
360C-220WP	4.63	50.6	92.2	85.7	1.32	1.92	70.5
360C-180WP-40MK	4.67	52	91.8	83	1.13	1.64	80.7
360C-180WP-40SF	4.625	50.6	97.8	91.1	1.04	1.49	81.9
320C-260WP	4.575	48.4	92.9	90.2	1.31	2.03	64.1
320C-220WP-40MK	4.61	49.9	93.4	86.4	1.31	1.78	68.4
320C-220WP-40SF	4.6	49.4	93.6	79.6	1.08	1.61	69.2

LF-based mixtures, reflecting the absence of pozzolanic activity and physical dilution of the hydrating matrix.

The $f'_{c(28d)}$ decreased progressively when the CEM content was reduced from 400 to 360 and 320 kg/m^3 (Figure 3). For example, $f'_{c(28d)}$ varied from 76.5 to 62.9 and 52.9 MPa for the 400C-180WP, 360C-220WP, and 320C-260WP mixtures, respectively. This can be directly related to reduced binding C_3S and C_2S compounds coupled with higher w/c (i.e., from 0.45 to 0.5 and 0.56) that could potentially attenuate hydration reactions and increase porosity in the hydrating system. Irrespective of the CEM content, the effect of incorporating MK or SF led to increased $f'_{c(28d)}$ due to pozzolanic reactions that produce hydrated phases and favor strength development [6, 17, 44]. The 400C-140WP-40MK yielded the highest $f'_{c(28d)}$ of 86.4 MPa.

Generally speaking, the $\Delta(f'_c)$ values for SCC mixtures prepared with 400 kg/m^3 CEM were pretty close to each other (Figure 3). On average, $\Delta(f'_c)$ determined after 600 days was 42% for WP-based mixtures, while this was 36% for LF-based mixtures. In contrast, however, the $\Delta(f'_c)$ significantly increased for mixtures prepared with reduced CEM content (i.e., 360 and 320 kg/m^3) together with higher WP concentration. For example, $\Delta(f'_c)$ reached 64% and 74% after 600 days for the 360C-220WP and 320C-260WP mixtures, respectively, containing 220 and 260 kg/m^3 WP, respectively. This can be attributed to a combination of phenomena including higher pozzolanic activity and certain amounts of mixing water absorbed by the WP materials that could promote hydration reactions and strength development over time [23, 26, 43].

The $f'_{c(600d)}$ reached 110.7 MPa for the 400C-180WP mixture, while this was only 79.5 MPa for the 400C-180LF mixture (Table 3), given the dilution effect that resulted from the presence of inert LF materials [12, 13]. Regardless of testing age, it is important to note that the f'_c values were always higher for mixtures containing combinations of WP together with MK and SF, as compared to SCC prepared with only WP (Table 3). The same trend was obtained for LF-based mixtures, which can be related to increased MK and SF fineness that improve pozzolanic reactions and refine the SCC microstructure [6, 17, 45]. Concurrently, several researchers proved the beneficial synergistic effects resulting from ternary binders (compared to binary ones) that foster nucleation effects and strength development [8, 10, 17].

Figure 4 plots the relationships between $f'_{c(28d)}$ with respect to those determined at various ages. At relatively early ages of 90 days, the average increase in compression was about 18%, with relatively high correlation coefficient (R^2) of 0.91. At longer ages of 400 and 600 days, the increase in compression hovers around 40% and 46%, respectively, but with relatively lower R^2 of 0.72 and 0.74, respectively.

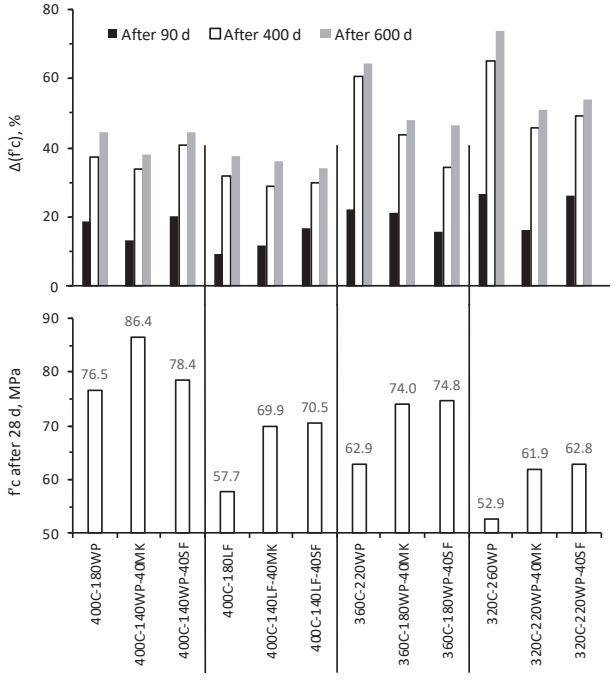

Figure 3. Effect of powder materials on f'_c at 28 days (lower part) and variation of $\Delta(f'_c)$ over testing age (upper part).

3.3. Water permeability tests

The W_{abs} and W_{depth} characteristics determined after 90 days for tested SCC are illustrated in Figure 5. Generally, mixtures prepared with increased cement content (i.e., having lower w/c) exhibited reduced water permeability; for example, W_{depth} decreased from 14.8 to 9.3 mm

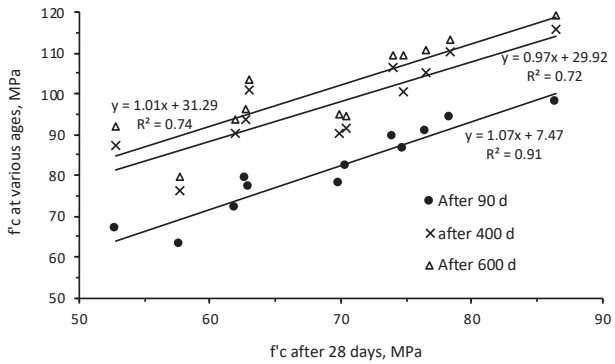

Figure 4. Relationships between f'_c determined at different ages.

for the 320C-260WP and 400C-180WP mixtures, respectively. This can mostly be associated to reduced w/c (i.e., from 0.56 to 0.45, respectively) that decreases the concrete capillary pores and average diameter [16, 46, 47].

Regardless of CEM content, the effect of incorporating MK or SF led to decreased water permeability (Figure 5). Such results are consistent with current literature, reflecting the marked influence of pozzolanic reactions on the compacity and denseness of the cementitious matrix, particularly at the interfacial transition zones with the fine and coarse aggregates [44, 45]. Silva and Brito [6] attributed the decrease in permeability of ternary binders to refinement of the cement paste microstructure through filling of pores by hydration products, making the system less interconnected and accessible to water permeation. Yet, it is interesting to note that the SF yielded consistently reduced water permeability, as compared to similar SCC containing MK. For example, W_{depth} dropped from 8.4 to 3.2 mm for the 400C-140WP-40MK and 400C-140WP-40SF mixtures, respectively. The corresponding W_{abs} determined at 90 days decreased from 2.72% to 1.75%, respectively. Similar results were reported by Meddah et al. [48] and Valipour et al. [49] who attributed such trends to different chemical composition (SiO_2 and Al_2O_3 ratios) and synergistic effects that alter the amount and size of capillary pores. For indication, it should be noted that the water permeability responses can be linked together, as shown in the following expressions:

$$W_{abs(650d)},\ \% = 0.72\ W_{abs(90d)}\ (\%) + 0.07 \quad R^2 = 0.7 \qquad \text{(Eq. 1)}$$

$$W_{depth(90d)},\ \text{mm} = 2.17\ W_{abs(90d)}\ (\%) + 2.64 \quad R^2 = 0.64 \qquad \text{(Eq. 2)}$$

Despite the LF inert nature, a remarkably low W_{abs} of 3.12% determined at 90 days was registered for the 400C-180LF mixture (as compared to 4.42% for equivalent SCC made with WP). Several researchers attributed the decrease in water permeability in LF-based mixtures to filling effect that reduces the spaces between cement particles and leads to better packing density [12, 13, 14]. Wu et al. [50] showed reduced porosity at the interfacial transition zones for ternary binders containing LF materials. Because of pozzolanic reactions and refinement of capillary pores, the addition of MK and SF significantly reduced W_{abs} to 1.84% and 1.72%, respectively, for the 400C-140LF-40MK and 400C-140LF-40SF mixtures, respectively.

Figure 6 plots typical relationships between the porosity determined after 400 days with respect to $f'_{c(400d)}$ and $W_{abs(650d)}$. Generally speaking, mixtures exhibiting higher porosity developed lower compressive strengths and increased vulnerability towards water permeability. The drop in $f'_{c(400d)}$ was from 115 to 75 MPa (i.e., by 35%) when the porosity increased from 6% to 11%. The corresponding drop in $W_{abs(650d)}$ was about two-folds higher (i.e., 70%), reflecting the impact of concrete porosity on water permeability. Good R^2 of 0.88 was obtained between porosity and $f'_{c(400d)}$. Yet, the R^2 decreased to 0.62 for $W_{abs(650d)}$, suggesting that concrete permeability is more related to the size and type of pores, rather than the total porosity in the system [16, 45, 47].

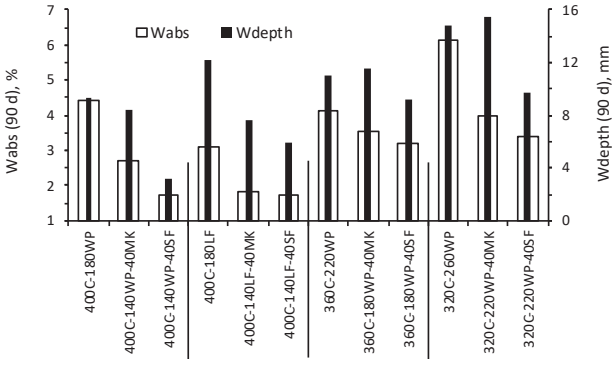

Figure 5. Effect of powder materials on the 90-days W_{abs} and W_{depth}.

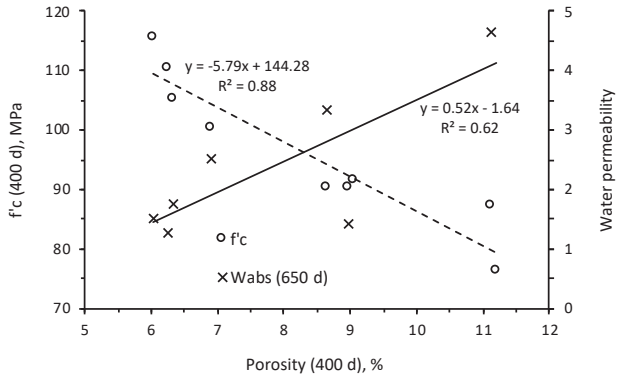

Figure 6. Relationships between porosity with respect to f'_c, W_{abs}, and W_{depth} determined at different ages.

3.4. Transport properties at various ages

Regardless of testing age, mixtures containing higher cement content (i.e., lower WP concentration) exhibited reduced carbonation depths and chloride migration coefficients. For example, as shown in Figure 7, D_{carb} after 400 days decreased from 3.24 to 3.14 and 2.41 mm for the 320C-260WP, 360C-220WP, and 400C-180WP mixtures, respectively. The corresponding D_{nssm} decreased from 4.15 to 3.81 and 2.63 $\times 10^{-12}$ m^2/s, respectively. As earlier explained, this can be related to the coupled effect of lower w/c (i.e., from 0.56 to 0.5 and 0.45, respectively) as well as reduced WP concentration in the concrete. From the other hand, the addition of MK or SF was beneficial to reduce D_{carb} and D_{nssm}, due to enhanced pozzolanic reactions and synergistic effects that refine the concrete microstructure and interfacial transition zones [6, 8, 51]. Moderate relationship with R^2 of 0.55 exists between porosity and D_{carb} measurements determined after 400 days; this can be expressed as:

$$D_{carb},\ \text{mm} = 0.162\ \text{Porosity}\ (\%) + 1.1 \quad R^2 = 0.55 \qquad \text{(Eq. 3)}$$

With some exceptions (Table 4), the 400C-180LF mixture exhibited relatively higher D_{carb} and D_{nssm} values (when compared to equivalent 400C-180WP mixture containing WP), suggesting that the filling effect associated with LF materials is insufficient to mitigate the transport properties. Earlier studies showed that the chloride ion penetrability is a complex process that does not solely depend on the matrix porosity, but rather involves other aspects such as CH content, diffusion, capillary suction, and migration in electrical field [12, 51, 52]. Yet, the combination of LF together with MK or SF showed significant drops in transport properties. For example, the D_{nssm} after 28 days decreased from 5.52 $\times 10^{-12}$ m^2/s for the 400C-180LF mixture to 3.71 and 2.52 $\times 10^{-12}$ m^2/s for the 400C-140LF-40MK and 400C-140LF-40SF mixtures, respectively. The relationships between $f'_{c(28d)}$ with respect to D_{carb} and D_{nssm}

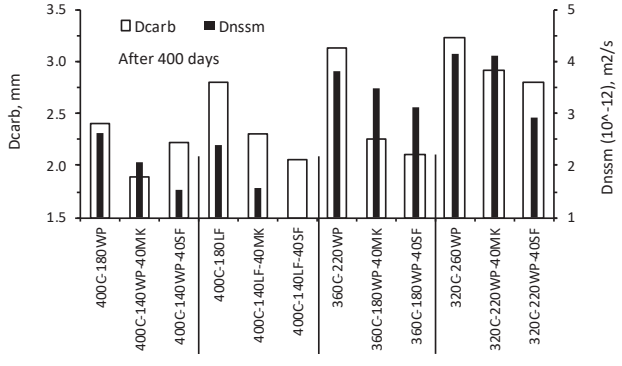

Figure 7. Effect of powder materials on D_{carb} and D_{nssm} determined after 400 days.

measurements determined after 28 days are given in Figure 8. Although moderate R^2 values (i.e., about 0.5), mixtures possessing higher compressive strengths are shown to exhibit better resistance against carbonation and chloride ion ingress.

The relationships between transport properties determined at different ages are plotted in Figure 9. At relatively early age of 28 days, good correlation having R^2 of 0.73 can be established, reflecting the interdependence of both properties on similar phenomena. The R^2 of relationships tended to decrease over time and resulting slopes become more and more flattened, reflecting the complex and synergistic effects taking place with elapsed times. The D_{nssm} values decreased by about 2-folds when measurements were conducted between 28 and 460 days, as a result of continued hydration reactions and refinement of concrete pores and microstructure. The increase in D_{carb} was remarkably higher (i.e., about 5-folds) during the same time span, which could be related to the continuous exposure of tested specimens to carbon dioxide. Typical relationships between D_{carb} and W_{abs} determined at different ages are plotted in Figure 10. As expected, mixtures exhibiting higher permeability due to increased porosity and/or presence of higher WP concentrations are susceptible to higher chloride ion attack.

3.5. Freeze and thaw cycles

Table 5 summarizes the ultrasonic pulse velocity determined before beginning F/T cycles (i.e., V_0) as well as the DF and cumulative mass loss determined after 300 and 400 cycles. The resulting dynamic modulus of elasticity for tested SCC varied roughly from 48 to 54 GPa; this was calculated as (Density$\times V_0^2$)/9.81. It is worth mentioning that V_0 responses tended to decrease for mixtures exhibiting higher porosity, reflecting the influence of voids on the ultrasonic pulse measurements. This relationship can be expressed as:

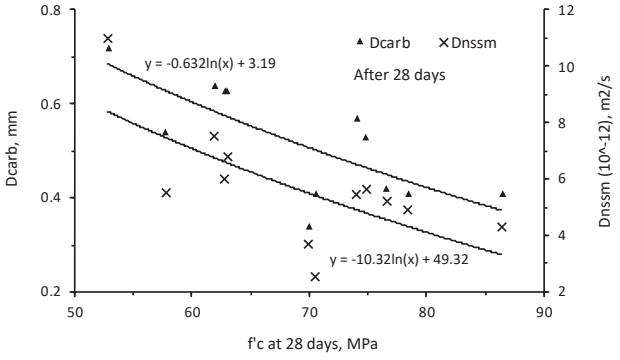

Figure 8. Relationships between f'_c with respect to D_{carb} and D_{nssm} (all being determined after 28 days).

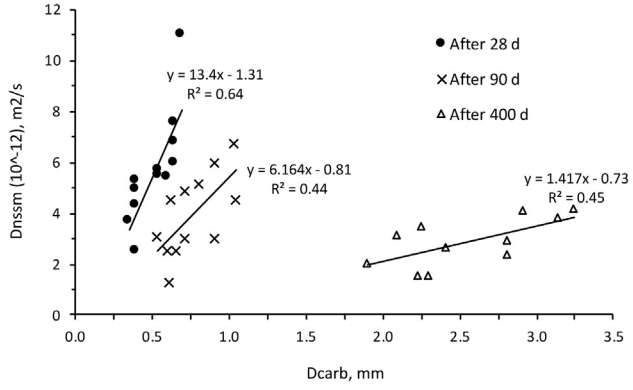

Figure 9. Relationships between D_{carb} and D_{nssm} determined at different ages.

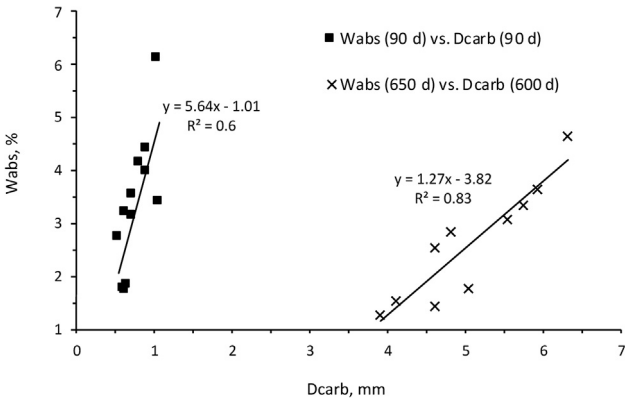

Figure 10. Relationships between D_{carb} and W_{abs} determined at different ages.

$$V_0, \text{ m/s} = -0.033 \times \text{Porosity (\%)} + 4.93 \quad R^2 = 0.53 \qquad \text{(Eq. 4)}$$

Typical DF variations for mixtures prepared with 400 kg/m^3 cement are plotted as a function of F/T cycles in Figure 11. Regardless of composition, all mixtures exhibited high resistance against freezing and thawing until 100 cycles; thereafter, the DF gradually decreased reflecting concrete deterioration caused by internal cracking of the cement paste, which grow larger with repeated cycles [53, 54]. The SCC containing WP together with 40 kg/m^3 SF showed marginal drop by 7%, while the highest drop of 33.5% corresponded to the mixture containing LF with 40% MK. The DF determined after given F/T cycles can be correlated to the cumulative mass loss, as follows:

$$\text{After 300 cycles: DF, \%} = -12.37 \times \text{Cum. mass loss (\%)} + 107.8 \quad R^2 = 0.62 \qquad \text{(Eq. 5)}$$

$$\text{After 400 cycles: DF, \%} = -15.89 \times \text{Cum. mass loss (\%)} + 112.1 \quad R^2 = 0.56 \qquad \text{(Eq. 6)}$$

Figure 12 summarizes the DF values determined after 400 cycles for various SCC. Generally, the effect of decreasing the cement content (i.e., increasing the WP concentration) led to increased resistance against F/T cycles. For example, the DF increased from 77.2% for the 400C-180WP mixture to 85.7% and 90.2% for the 360C-220WP and 320C-260WP mixtures, respectively. This can mostly be related to the WP pozzolanic activity that refines the concrete microstructure and contributes in accommodating the disruptive expansive stresses due to frost attack. Such observation is in line with the pressure dissipation theory due to porous structure of adhered mortar when using recycled aggregates [42, 53, 55]. Bektas et al. [26] reported that the porous structure of both natural and expanded perlite provides closely distributed air bubbles that relief potential pressure and suppress the deleterious alkali-silica expansive reactions.

As shown in Figure 12, the LF-based mixtures prepared with 400 kg/m^3 cement behaved quite similarly to equivalent ones containing WP. The substitution of 40 kg/m^3 WP by SF led to improvement in DF, which can be attributed to pozzolanic reactions that create denser microstructure and interfacial transition zones [10, 44, 50]. For example, this varied from 77.2% to 93.1% for the 400C-180WP and 400C-140P-40SF mixtures, respectively. Mixtures containing MK and 400 kg/m^3 cement exhibited the least resistance against frost attack; the resulting DF was 67.4% and 66.5% for the 400C-140WP-40MK and 400C-140LF-40MK mixtures, respectively.

As noted in the experimental program, the 150-mm cubic specimens used for F/T testing were crushed in compression after the last cycle (i.e., cycle number 400). Figure 13 plots the relationships between the resulting drop in f'_c determined after 90 days with respect to DF and cumulative mass loss. Clearly, the higher the drop in f'_c, the lower is DF and higher is the cumulative mass loss. The drop in DF followed a logarithmic variation with high R^2 of 0.91, while moderate R^2 of 0.61 was obtained with the cumulative mass loss.

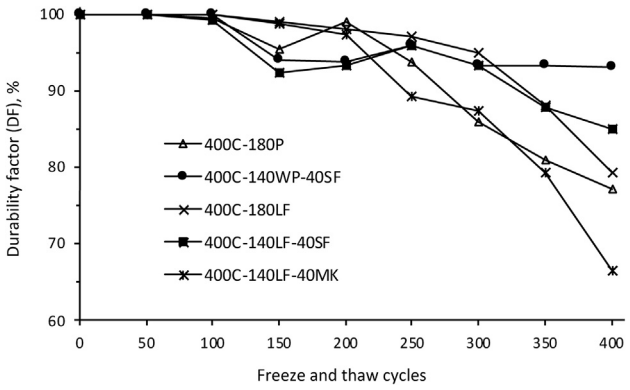

Figure 11. Typical variations of DF with F/T cycles.

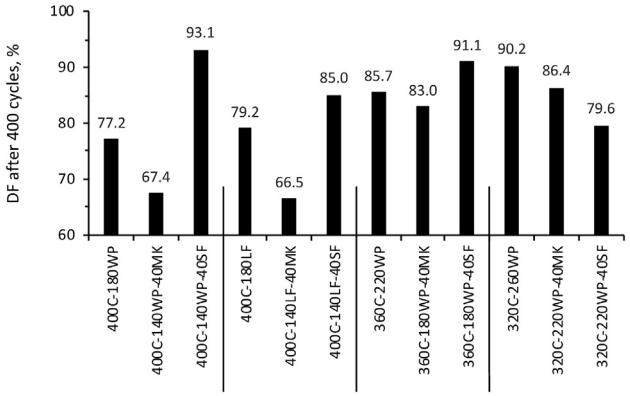

Figure 12. Effect of powder materials on DF determined after 400 cycles.

4. Annex

Statistical analysis is widely used in materials science to elaborate predictive models and facilitate optimization of a single or group of variables (or, predictors) on performance of cementitious composites [1, 56, 57]. Series of linear regression models are proposed in Eqs. (7), (8), (9), and (10) for predicting SCC compressive strength, at specified age. The models are valid for mixtures having 580 kg/m^3 powder content and 0.31 w/p; the predictors including CEM, WP, LF, MK, and SF varied from 320 to 400 kg/m^3, 140–260 kg/m^3, 140–260 kg/m^3, 0–40 kg/m^3, and 0–40 kg/m^3, respectively (a total of 34 data points were considered from [20, 22] and current paper). The weights of predictors were optimized by minimizing the squared deviations of measured-to-predicted responses from the regression fit line. The R^2 that resulted from the relationships of

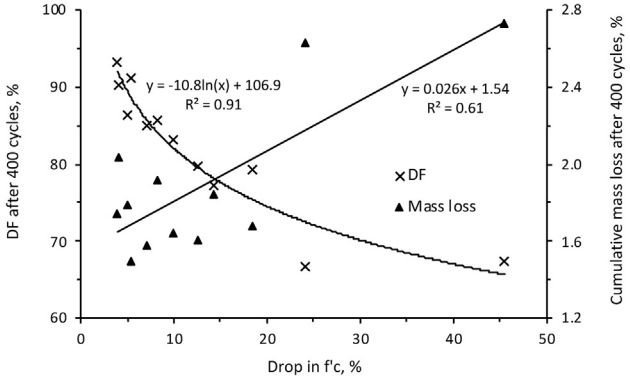

Figure 13. Relationships between the drop in f'_c with respect to DF and cumulative mass loss determined after 400 cycles.

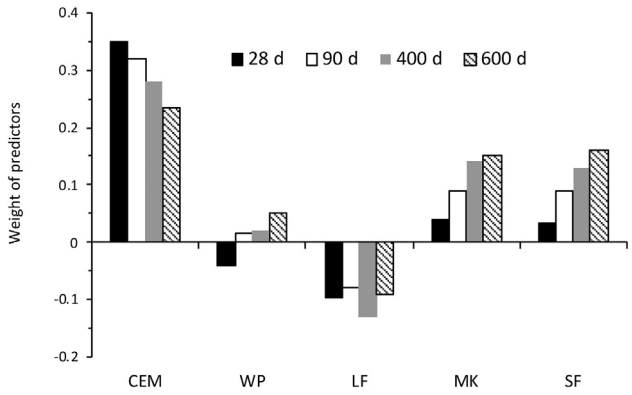

Figure 14. Variations of predictor weights with powder type and testing age when assessing f'_c at various ages.

the predicted-to-measured responses varied from 0.81 to 0.94, indicating acceptable to high accurate models.

$$f'_{c(28d)}, \text{MPa} = 0.35\,\text{CEM} - 0.04\,\text{WP} - 0.096\,\text{LF} + 0.038\,\text{MK} + 0.033\,\text{SF} - 49.1 \quad (R^2 = 0.81) \qquad \text{(Eq. 7)}$$

$$f'_{c(90d)}, \text{MPa} = 0.32\,\text{CEM} + 0.015\,\text{WP} - 0.08\,\text{LF} + 0.09\,\text{MK} + 0.09\,\text{SF} - 34 \quad (R^2 = 0.83) \qquad \text{(Eq. 8)}$$

$$f'_{c(400d)}, \text{MPa} = 0.28\,\text{CEM} + 0.02\,\text{WP} - 0.13\,\text{LF} + 0.14\,\text{MK} + 0.13\,\text{SF} - 4 \quad (R^2 = 0.92) \qquad \text{(Eq. 9)}$$

$$f'_{c(600d)}, \text{MPa} = 0.235\,\text{CEM} + 0.05\,\text{WP} - 0.09\,\text{LF} + 0.15\,\text{MK} + 0.16\,\text{SF} + 8.3 \quad (R^2 = 0.94) \qquad \text{(Eq. 10)}$$

It is interesting to note that the predictors relative weights and signs (±) could be used to assess the major trends and influence of given powder on performance of SCC. For example, as shown in Figure 14, the relative weight attributed to CEM gradually decreased over testing age, reflecting reduced contribution of cement effect on strength development at longer ages. The opposite trend occurred for SF and MK, due to their pozzolanic activities. From the other hand, the predictor signs (±) reflect their positive or negative influence on SCC performance. For instance, an increase in the CEM, SF, or MK content led to an increase (+) in f'_c, while conversely, the addition of LF decreased (–) f'_c (Figure 14). At early age (i.e., 28 days), the WP was assigned a negative sign reflecting a decreased effect on f'_c, while this turned positive at longer ages given the pozzolanic and self-curing properties.

5. Conclusions

The main objective of this paper is to evaluate the effect of WP along with its combination with LF, MK, and SF on durability and long-term transport properties of SCC. Based on foregoing, the following conclusions can be warranted:

- SCC containing WP exhibited remarkably higher f'_c than equivalent mixtures prepared using LF, which was attributed to different powder physico-chemical compositions and properties. The WP is an alumino-silicate rich powder that reacts with Portlandite during cement hydration, while LF is a chemically inert filler.
- Irrespective of the cement content and testing age, the f'_c was consistently higher for SCC containing combinations of WP together with MK and SF, as compared to mixtures prepared with only WP. This was related to a combination of phenomena including increased MK and SF fineness that help promoting the pozzolanic reactions and refining the SCC microstructure. The evolution of f'_c over time significantly increased for SCC prepared with higher WP concentration.

- Mixtures prepared with increased cement content, lower w/c, and/or containing lower WP concentration exhibited reduced water permeability (i.e., W_{abs} and W_{depth}) and transport properties (i.e., D_{carb} and D_{nssm}). Also, the substitution of 40 kg/m^3 WP by MK or SF led to decreased water and chloride ions permeations, reflecting the marked influence of pozzolanic reactions on refinement of the paste-aggregate interfacial transition zones. Moderate relationships were established between porosity with respect to water permeability and transport properties.
- The incorporation of LF led to decreased water permeability, given the filling effect that improved packing density by reducing the spaces between cement particles. However, the LF was not efficient to reduce the migration of chloride ions, given the complexity associated to transport processes.
- The resistance against F/T cycles improved when SCC mixtures are prepared with higher WP concentration. In addition to pozzolanic reactions, this was partly attributed to the porous WP nature that helps reducing the disruptive expansive stresses, just like what happens with lightweight and recycled aggregates. The substitution of 40 kg/m^3 WP by SF led to improved resistance against F/T cycles.

Declarations

Author contribution statement

Abdulkader El Mir, Salem G. Nehme & Joseph J. Assaad: Conceived and designed the experiments; Performed the experiments; Analyzed and interpreted the data; Contributed reagents, materials, analysis tools or data; Wrote the paper.

Funding statement

This research did not receive any specific grant from funding agencies in the public, commercial, or not-for-profit sectors.

Competing interest statement

The authors declare no conflict of interest.

Additional information

No additional information is available for this paper.

References

[1] A. Ghezal, K.H. Khayat, Optimizing self-consolidating concrete with limestone filler by using statistical factorial design methods, ACI Mater. J. 99 (3) (2002) 264–272.
[2] J. Assaad, K.H. Khayat, Effect of casting rate and concrete temperature on formwork pressure of self-consolidating concrete, Mater. Struct. 39 (3) (2006) 333–341.
[3] S.G. Nehme, Influence of supplementary cementing materials on conventional and self- compacting concretes. Part 1. Literature review, Epitoanyag J. Silicate Based Compos. Mater. 67 (2015) 28–33.
[4] H. Mohammed, M.A.S. Arab, A.I. El-Kassas, Behavior of high strength self compacted concrete deep beams with web openings, Heliyon 5 (4) (2019).
[5] C. Issa, J. Assaad, Stability and bond properties of polymer-modified self-consolidating concrete for repair applications, Mater. Struct. 50 (28) (2017) 1–16.
[6] P.R. da Silva, J. de Brito, Experimental study of the porosity and microstructure of self-compacting concrete (SCC) with binary and ternary mixes of fly ash and limestone filler, Constr. Build. Mater. 86 (2015) 101–112.
[7] A. Noaman, R. Karim, N. Islam, Comparative study of pozzolanic and filler effect of rice husk ash on the mechanical properties and microstructure of brick aggregate concrete, Heliyon 5 (6) (2019).
[8] S. Sujjavanich, P. Suwanvitaya, D. Chaysuwan, G. Heness, Synergistic effect of metakaolin and fly ash on properties of concrete, Constr. Build. Mater. 155 (2017) 830–837.
[9] W.Z. Zhu, P.J.M. Bartos, Permeation properties of SCC, Cem. Concr. Res. 33 (6) (2003) 921–926.
[10] S.-D. Hwang, K.H. Khayat, Durability characteristics of self-consolidating concrete designated for repair applications, Mater. Struct. 42 (2009) 1–14.
[11] J. Assaad, K.H. Khayat, Kinetics of formwork pressure drop of self-consolidating concrete containing various types and contents of binder, Cement Concr. Res. 35 (2005) 1522–1530.
[12] D. Wang, C. Shi, N. Farzadnia, Z. Shi, H. Jia, A review on effects of limestone powder on the properties of concrete, Constr. Build. Mater. 192 (2018) 153–166.
[13] E.T. Dawood, Y.Z. Mohammad, W.A. Abbas, M.A. Mannan, Toughness, elasticity and physical properties for the evaluation of foamed concrete reinforced with hybrid fibers, Heliyon 4 (12) (2018).
[14] N. Ghafoori, R. Spitek, M. Najimi, Influence of limestone size and content on transport properties of self-consolidating concrete, Constr. Build. Mater. 127 (2016) 588–595.
[15] M. Antoni, J. Rossen, F. Martirena, K. Scrivener, Cement substitution by a combination of metakaolin and limestone, Cem. Concr. Res. 42 (12) (2012) 1579–1589.
[16] G. Ye, X. Liu, G. De Schutter, A.-M. Poppe, L. Taerwe, Influence of limestone powder used as filler in SCC on hydration and microstructure of cement pastes, Cement Concr. Compos. 29 (2) (2007) 94–102.
[17] G. Medjigbodo, E. Rozière, K. Charrier, L. Izoret, A. Loukili, Hydration, shrinkage, and durability of ternary binders containing Portland cement, limestone filler and metakaolin, Constr. Build. Mater. 183 (2018) 114–126.
[18] T. Markiv, K. Sobol, M. Franus, W. Franus, Mechanical and durability properties of concrete incorporating natural zeolite, Arch. Civil Mech. Eng. 16 (4) (2016) 554–562.
[19] A.M. Rashad, A synopsis about perlite as building material - a best practice guide for Civil Engineer, Constr. Build. Mater. 121 (2016) 338–353.
[20] A. El Mir, Influence of Additives on the Porosity-Related Properties of Self-Compacting concrete, Ph.D. thesis, Budapest University of Technology and Economics, Faculty of Civil Engineering, 2018.
[21] D. Okuyucu, L. Turanli, B. Uzal, T. Tankut, Some characteristics of fibre reinforced semi-lightweight concrete containing unexpanded perlite both as aggregate and as a supplementary cementing material, Mag. Concr. Res. 63 (2001) 1–10.
[22] A. El Mir, S.G. Nehme, Utilization of industrial waste perlite powder in self-compacting concrete, J. Clean. Prod. 156 (2017) 507–517.
[23] R. Demirboğa, I. Örüng, R. Gül, Effects of expanded perlite aggregate and mineral admixtures on the compressive strength of low-density concretes, Cem. Concr. Res. 31 (2001) 1627–1632.
[24] T.K. Erdem, C¸. Meral, M. Tokyay, T.Y. Erdoğan, Use of perlite as a pozzolanic addition in producing blended cements, Cement Concr. Compos. 29 (2007) 13–21.
[25] A.A. Ramezanianpour, S.M. Motahari Karein, P. Vosoughi, A. Pilvar, S. Isapour, F. Moodi, Effects of calcined perlite powder as a SCM on the strength and permeability of concrete, Constr. Build. Mater. 66 (2014) 222–228.
[26] F. Bektas, L. Turanli, P.J.M. Monteiro, Use of perlite powder to suppress the alkali-silica reaction, Cem. Concr. Res. 35 (2005) 2014–2017.
[27] L.H. Yu, H. Ou, L.L. Lee, Investigation on pozzolanic effect of perlite powder in concrete, Cem. Concr. Res. 33 (2003) 73–76.
[28] M. Jamei, H. Guiras, Y. Chtourou, A. Kallel, E. Romero, I. Georgopoulos, Water retention properties of perlite as a material with crushable soft particles, Eng. Geol. 122 (2011) 261–271.
[29] J. Assaad, C. Issa C., Use of locked-cycle protocol to assess cement fineness and properties in laboratory-grinding mills, ACI Mater. J. 113 (4) (2016) 429–438.
[30] BS EN ISO 17892-3, Geotechnical Investigation and Testing - Laboratory Testing of Soil - Part 3 Determination of Particle Density, 2014, p. 20.
[31] K.H. Khayat, J.J. Assaad, Use of thixotropy-enhancing agent to reduce formwork pressure exerted by self-consolidating concrete, ACI Mater. J. 105 (1) (2008) 88–96.
[32] J. Assaad, Y. Daou, Cementitious grouts with adapted rheological properties for injection by vacuum techniques, Cement Concr. Res. 59 (2014) 43–54.
[33] EPG (Self-Compacting Concrete European Project Group), Guidelines for Self-Compacting concrete, Specification, Production and Use, 2005. See, http://www.ermco.eu/document/scc_guidelines_may_2005_final-pdf.
[34] BS, Testing Hardened Concrete, Compressive Strength of Test Specimens, European Standard, 2019. EN12390-3:2009.
[35] ASTM, Standard Test Method for Density, Absorption, and Voids in Hardened Concrete, American Society for Testing and Materials, United States, 2013. ASTM C642-2013.
[36] BS, Testing concrete, Method for Determination of Water Absorption, European Standard, 2011. EN 1881-122:2011.
[37] BS, Testing Hardened Concrete, Depth of Penetration of Water Under Pressure, European Standard, 2019. EN 12390- 8:2009.
[38] CPC-18 Measurement of hardened concrete carbonation depth, Mater. Struct. 21 (1988) 453–455.
[39] NT BUILD 492, Concrete, Mortar and Cement-Based Repair Materials: Chloride Migration Coefficient from Non-steady-state Migration Experiments, Nordtest Method UDC 691 (1999) 8. Approved 1999-11, http://www.nordtest.info.
[40] CEN, Testing the Freeze-Thaw Resistance of concrete – Internal Structural Damage, CEN/TR 15177:2006, 2006. Technical Report, Technical Committee CEN/TC 51.
[41] CEN EN 12504–2:2012, Testing concrete in Structures – Part 2: Nondestructive Testing – Determination of Rebound Number, European Standard, 2012.
[42] J.J. Assaad, Y. Daou, Behavior of structural polymer-modified concrete containing recycled aggregates, J. Adhes. Sci. Technol. 31 (8) (2017) 874–896.
[43] J.J. Assaad, N. Gerges, C. Issa, Bond to reinforcement of polymeric lightweight flowable concrete for structural applications, J. Adhes. Sci. Technol. 33 (6) (2019).
[44] E. Güneyisi, M. Gesoglu, S. Karaoglu, K. Mermerdas, Strength, permeability and shrinkage cracking of silica fume and metakaolin concretes, Constr. Build. Mater. 34 (2012) 120–130.
[45] M. Uysal, K. Yilmaz, M. Ipek, The effect of mineral admixtures on mechanical properties, chloride ion permeability and impermeability of self-compacting concrete, Constr. Build. Mater. 27 (1) (2012) 263–270.
[46] M.J. Mwiti, T.J. Karanja, W.J. Muthengia, Properties of activated blended cement containing high content of calcined clay, Heliyon 4 (8) (2018).

[47] C. Lian, Y. Zhuge, S. Beecham, The relationship between porosity and strength for porous concrete, Constr. Build. Mater. 25 (11) (2011) 4294–4298.
[48] M.S. Meddah, M.A. Ismail, S. Gamal, H. Fitriani, Performances evaluation of binary concrete designed with silica fume and metakaolin, Constr. Build. Mater. 166 (2018) 400–412.
[49] M. Valipour, F. Pargar, M. Shekarchi, S. Khani, Comparing a natural pozzolan, zeolite, to metakaolin and silica fume in terms of their effect on the durability characteristics of concrete: a laboratory study, Constr. Build. Mater. 41 (2013) 879–888.
[50] K. Wu, H. Shi, L. Xu, G. Ye, G. De Schutter, Microstructural characterization of ITZ in blended cement concretes and its relation to transport properties, Constr. Build. Mater. 79 (2016) 243–256.
[51] V.G. Papadakis, Effect of supplementary cementing materials on concrete resistance against carbonation and chloride ingress, Cem. Concr. Res. 30 (2) (2000) 291–299.
[52] M.R. Jones, R.K. Dhir, B.J. Magee, Concrete containing ternary blended binders: resistance to chloride ingress and carbonation, Cem. Concr. Res. 27 (1997) 825–831.
[53] R. Kurda, J.D. Silvertre, J. de Brito, Toxicity and environmental and economic performance of fly ash and recycled concrete aggregates use in concrete: a review, Heliyon 4 (4) (2018).
[54] J.A. Bogas, J. de Brito, D. Ramos, Freeze-thaw resistance of concrete produced with fine recycled concrete aggregates, J. Clean. Prod. 115 (2016) 294–306.
[55] M.V. Lizancos, I.M. Lage, P.V. Burgo, The effect of recycled aggregates on the accuracy of the maturity method on vibrated and self-compacting concretes, Arch. Civil Mech. Eng. 19 (2) (2019) 311–321.
[56] G.P. Zehil, J.J. Assaad, Feasibility of concrete mixtures containing cross-linked polyethylene waste materials, Constr. Build. Mater. 226 (2019) 1–10.
[57] J.J. Assaad, P. Matar, Regression models to predict SCC pressure exerted on formworks containing vertical and transverse reinforcing bars, Mater. Struct. 51 (3) (2018).